metals

MDPI

Article

Effect of Aging Treatment on the Mechanical Properties and Impact Abrasive Wear Property of High-Manganese Steel

Xiya Qiao [1,2], Ling Yan [3], Xiao Han [1,2,*], Xiangyu Qi [3], Xin Yang [1,2] and Yu Xin [1,2]

[1] School of Materials and Metallurgy, University of Science and Technology Liaoning, Anshan 114051, China; qxy5272021@163.com (X.Q.); 15841693946@163.com (X.Y.); xy1173259002@163.com (Y.X.)
[2] Key Laboratory of Green Low-Carbon and Intelligent Metallurgy Liaoning Province, Anshan 114051, China
[3] State Key Laboratory of Metal Material for Marine Equipment and Application, Anshan 114009, China; yanling_1101@126.com (L.Y.); qixiangyu881029@163.com (X.Q.)
* Correspondence: tophanxiao@126.com

Abstract

High manganese steel can improve its microstructure after aging treatment, which is beneficial for enhancing strength, toughness, and wear resistance. This study aims to explore the effect of aging treatment on mechanical properties and wear resistance of high manganese steel (containing 25% Mn, called Mn25 steel) by designing different aging temperatures (450 °C, 500 °C, and 550 °C) with the same aging time (1 h). The results indicated that with the increase in aging treatment temperature, the surface hardness of Mn25 steel first increased and then decreased, but was still higher than that of untreated Mn25 steel. In addition, the impact toughness of steel decreased first and then increased with the increase in aging temperature, with the optimal hardness and impact toughness exhibited at 550 °C. The impact abrasive wear test results showed that the weight loss of Mn25 steel decreased with the increase in aging treatment temperature. After aging treatment at 550 °C, the weight loss is the lowest, which shows the optimal wear resistance performance. Under a high-impact load of 5.0 J, the hardness increased by nearly 49.96% after impact abrasive wear, and the effective hardening layer of the steel was the thickest, about 3800 μm. This is mainly related to the best match between the hardness and impact toughness of high manganese steel after aging treatment. The wear morphology is often caused by various wear mechanisms working together to cause the wear loss of Mn25 steel during the impact wear process. The wear morphologies of the Mn25 steel were mainly characterized by press-in particles, furrow, spalling, and strain fatigue. Through experimental analysis, a suitable aging treatment process has been determined, providing a theoretical basis for the practical application of high manganese steel.

Keywords: high manganese steel; aging treatment; aging temperature; mechanical properties; impact abrasive wear

Academic Editor: Andrea Di Schino

Received: 12 June 2025
Revised: 10 August 2025
Accepted: 13 August 2025
Published: 16 August 2025

Citation: Qiao, X.; Yan, L.; Han, X.; Qi, X.; Yang, X.; Xin, Y. Effect of Aging Treatment on the Mechanical Properties and Impact Abrasive Wear Property of High-Manganese Steel. *Metals* **2025**, *15*, 909. https://doi.org/10.3390/met15080909

1. Introduction

High manganese steel is widely used in mining machinery, railway turnouts, and other working conditions under high-impact load because of its excellent work-hardening ability and impact wear resistance [1–3]. However, in the process of dynamic wear, the material surface is prone to fatigue spalling due to repeated impact, which leads to a reduction in service life. For this reason, researchers have employed diverse strategies to optimize the mechanical properties and wear resistance of high-manganese steel, including microalloying or re-alloying [4–7], pre-hardening treatments [8–11], and heat treatment [12–18].

Wang et al. [11] studied the effects of surface impact parameters on the performance of pre-hardened high-manganese steel samples. The results revealed that impact hardening increased the hardness of the top surface within a certain depth. In addition, the tested steel exhibited good wear resistance after surface impact hardening. However, excess impact induced microcracking along the top surface, resulting in deteriorated wear resistance. Lee at al. [14] found that when the aging temperature is 550 °C, the Vickers hardness of high-manganese steel increased with the aging time. Feng et al. [15] also found that after aging at 550 °C, the hardness exhibited a continuous increase with the aging time and, finally, stabilized around 480 HB. Shin J H et al. [16] found that k-carbide precipitated within grain and on grain boundary during aging heat-treatment improved yield strength and ultimate tensile strength, and reduced percentage elongation to fracture; for the aging specimen, the fractography showed that the fracture type changed from intergranular fracture with slip band and dimples to trans-granular fracture with dimples as test temperature increased. Shan et al. [17] found that the volume fraction of precipitates increased with aging treatment temperature. In addition, when the aging temperatures are higher than 450 °C, Young's modulus and nano-hardness of the high-manganese steel are significantly enhanced, and the overall Vickers hardness is also improved, which is mostly related to the precipitation strengthening of precipitates. Ren J et al. [18] found that when the aging temperature is at 800 °C, there is a pronounced increment of 100 MPa in both yield and tensile strengths. Although previous studies have extensively investigated the use of aging treatment processes to enhance the mechanical properties and wear resistance of high-manganese steel, the effects of the aging treatment were different for different alloy systems of high-manganese steels. Additionally, there are few reports on the impact wear behavior of cast high-manganese steel with a high manganese content of 25%.

In this study, the effects of aging treatment temperature on mechanical properties, and impact abrasive wear property of high-manganese steel (called Mn25 steel) were systematically investigated, providing a theoretical basis for optimizing the heat treatment process parameters of high-manganese steel and offering new insights into improving the performance of novel high-manganese austenitic steels.

2. Experimental

The Mn25 steel was melted by a laboratory vacuum high-frequency induction furnace in this work, and the actual chemical compositions were measured by direct-reading spectrometer (QSN750, OBLF Co., Ltd., Witten, Germany) and cast into test pieces. The chemical compositions of the sample studied are given in Table 1.

Table 1. The chemical compositions of the investigated high-manganese steel.

Elements	C	Si	Mn	Cr	Ni	Cu	Mo	P	S	Al	Fe
Weight (wt%)	0.35	0.15	24.98	3.58	0.014	0.48	0.0079	0.007	0.0083	0.009	Balance

The test sample was prepared via the wire cutting mechanism. Specimens with dimensions of 150 mm × 22 mm × 40 mm were solution-treated at 1050 °C for 0.5 h and then water-quenched. After solution treatment, the specimens were aged at 450 °C, 500 °C, and 550 °C for 1 h, respectively. The processing diagram of the aging treatment of the specimens is as shown in Figure 1.

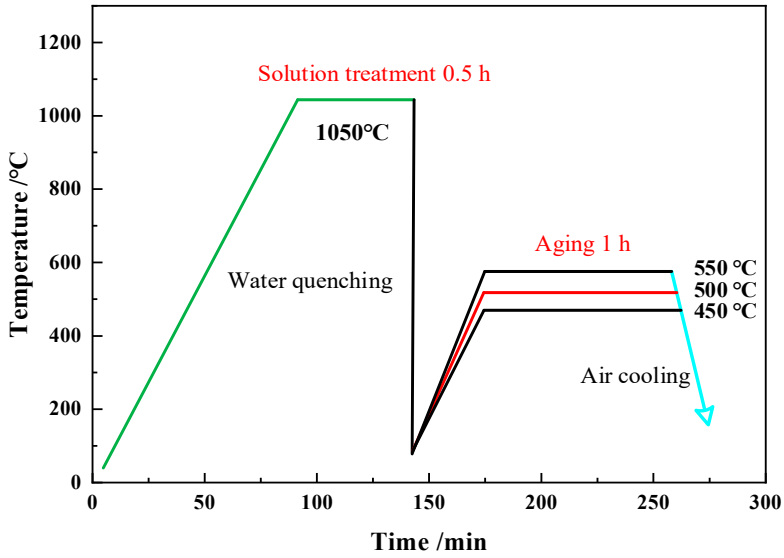

Figure 1. Processing diagram of the aging treatment of the specimens.

Surface hardness of the steel before and after the impact wear test were tested by a micro-Vickers hardness machine (HV-1000, Jinan Liling Testing Machine Co., Ltd., Jinan, China). Each sample was randomly selected to measure the hardness at 5 points, and the average value was taken as the final hardness value. Charpy impact tests were carried out in accordance with the GB/T 229-2020 standard [19]. All test samples were 10 mm × 10 mm × 55 mm and were taken from the center area of the original steel sample, and the test temperature was 25 ± 0.5 °C. To ensure the accuracy of the test results, each group of tests was repeated at least 3 times, and the results were average. Scanning electron microscope (SEM, ZEISS Sigma 560, Oberkochen, Germany) was used to observe morphologies of impact fracture surface.

After the 15 mm × 15 mm × 10 mm samples were washed with deionized water and anhydrous ethanol for 5 min, they were placed in a drying dish for later use. The remaining surfaces, except for the 15 mm × 15 mm working surface, were sealed with epoxy resin. Phase identification was performed via X-ray diffraction (XRD, D8 ADVANCE, Karlsruhe, Germany) with a Cu-K_α target. The scanning rate and range of XRD analysis were 2°/min and 20~100°, respectively.

The impact wear tests were conducted with MLD-10 impact wear testing machine (Shandong Hongde Industrial Co., Ltd., Jining, China) (as shown in Figure 2a). The impact wear tests were performed under low-energy impact (2.0 J) and high-energy impact (5.0 J), respectively. The upper specimens were the investigated steels with dimensions of 10 mm × 10 mm × 30 mm (as shown in Figure 2b). Pre-grinding of the specimen before the wear test is 20 min, in order to eliminate the upper and lower specimens of the assembly error and other factors; after the end of the pre-grinding of the specimen, ultrasonic cleaning → drying → weighing was performed, marking the mass at this time for M_0 (i.e., the official wear test of the initial mass). The specimen was removed every 20 min, cleaned, dried, and weighed once, and recorded as M_i (i = 1, 2, 3, 4). The difference between the initial weight M_0 and M_i is considered to be the loss of weight of the specimen during a given wear time. To characterize the wear mechanism of high manganese steel, scanning electron microscope (SEM) was used to observe the wear morphology of the impacted abrasive wear specimens.

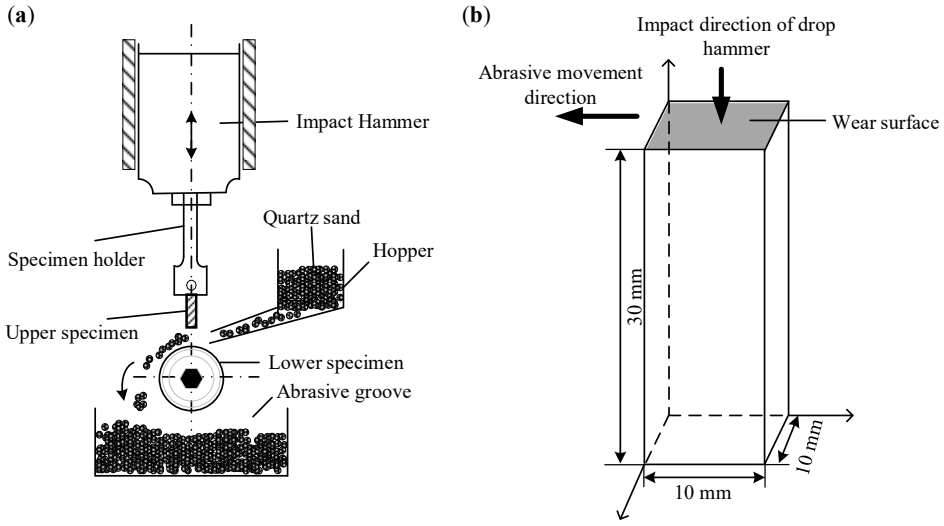

Figure 2. The MLD-10 machine: (**a**) work diagram; and (**b**) size diagram of impact wear test specimen.

3. Results and Discussion

3.1. Effect of Aging Temperature on Mechanical Properties of High Manganese Steel

The effects of different aging temperatures on the hardness and impact toughness of Mn25 steel are shown in Figure 3. As can be seen in Figure 3, the surface hardness of Mn25 steel was improved after aging treatment. When the aging temperature is 400 °C, the surface hardness of Mn25 steel reaches the maximum value (331.16 HV), and then the surface hardness decreases with the aging temperature increase. And the impact toughness of Mn25 steel, with the aging temperature, at first sharply decreased and then increased. When the aging temperature continues to rise, the austenite matrix rises along with the crystal precipitation carbides, resulting in a reduction in the toughness of the Mn25 steel. At the aging temperature of 500 °C, the impact toughness performance of Mn25 steel reaches the maximum value, which is 199.68 J. When at the aging temperature of 450 °C, the impact toughness of Mn25 steel value is the smallest (153.92 J). When the aging temperature is 550 °C, the impact toughness and hardness match better. Comprehensive analysis, the purpose of aging treatment is to eliminate the internal stresses of Mn25 steel; the precipitation phase is uniformly dispersed precipitation in the matrix, which can improve the initial hardness of high manganese steel, while the toughness is not reduced [20].

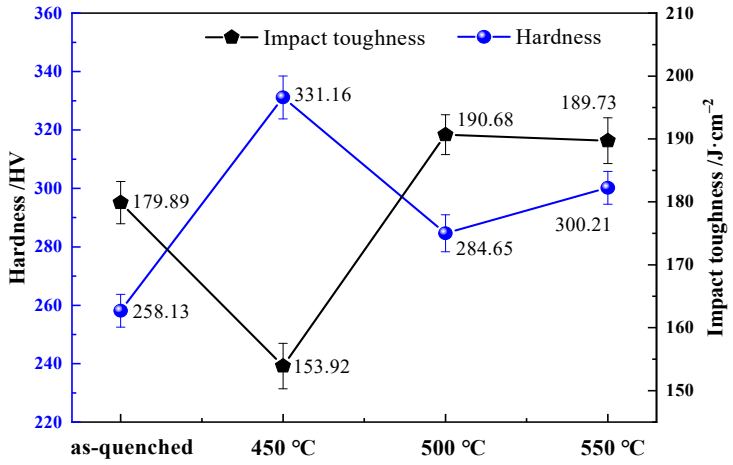

Figure 3. Hardness and impact toughness of Mn25 steel at different aging temperatures.

Figure 4 shows that morphologies of the impact fracture surface of Mn25 steel under different aging temperatures. As can be seen in Figure 4a,b, the surface of the fracture is rough, which is mainly characterized by irregularly distributed holes and elongated tear edges. The fracture surface is covered with evenly distributed deep truncated holes and the edges of the truncated holes are smooth, indicating that the material undergoes significant plastic deformation during fracture. As can be seen in Figure 4c,d, when the aging temperature is 450 °C, the fracture surface mainly coexists with large-size deep tough holes and small shallow holes, with significantly uneven distribution. When the aging temperature is 500 °C (Figure 4e,f), the fracture is dominated by a uniformly distributed deep dimple, indicating its excellent plastic deformation ability and energy absorption ability. The fracture has no cleavage surface, and the tear edges are round and blunt, which confirms that the brittle fracture mechanism is effectively suppressed. When the aging temperature continued to rise to 550 °C, there were some cracks and large dimples on the fracture surface, tiny holes gathered locally, and obvious shear bands on the edges (Figure 4g,h). Carbide precipitation is present from the matrix to needle carbide, which is favorable to improve the hardness of high manganese steel, and, at the same time, produce new heat treatment stress, and induce cracks, resulting in high manganese steel impact toughness decline [17]. This is consistent with the results of impact tests in this work.

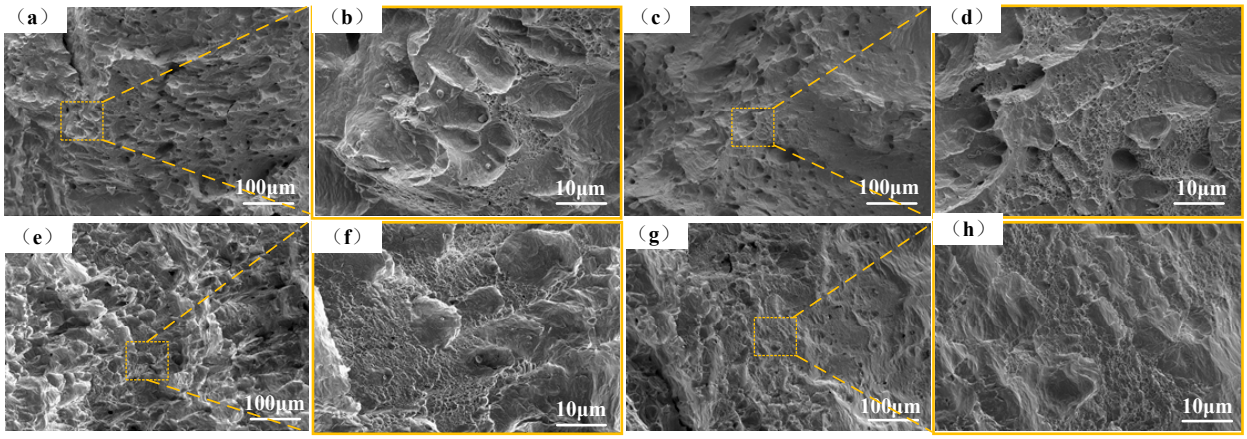

Figure 4. Morphologies of the impact fracture surface of Mn25 steel under different aging temperatures. (**a**,**b**) as-quenched, (**c**,**d**) 450 °C, (**e**,**f**) 500 °C, and (**g**,**h**) 550 °C.

3.2. Effect of Aging Temperature on X-Ray Diffraction Analysis of High-Manganese Steel

To further study the relationship between the composition of precipitates and their mechanical properties of high manganese steel after aging treatment, X-ray diffraction analysis was carried out on Mn25 steel after treatment at different aging temperatures, and the results are shown in Figure 5. The post-water-quenching treatment of the organization of Mn25 steel for austenite can be seen in Figure 5. When at the aging temperature of 450 °C, the matrix organization of Mn25 steel is still austenite, and at the same time the carbide $(Mn, Fe)_3C$ diffraction peak appeared, indicating the austenite precipitation of $(Mn, Fe)_3C$ carbides at this time. Subsequently, at the aging temperature of 500 °C, $(Mn, Fe)_3C$ carbide diffraction peaks gradually become weaker. When at the aging temperature of 550 °C, $(Mn, Fe)_3C$ carbide diffraction peaks gradually become stronger.

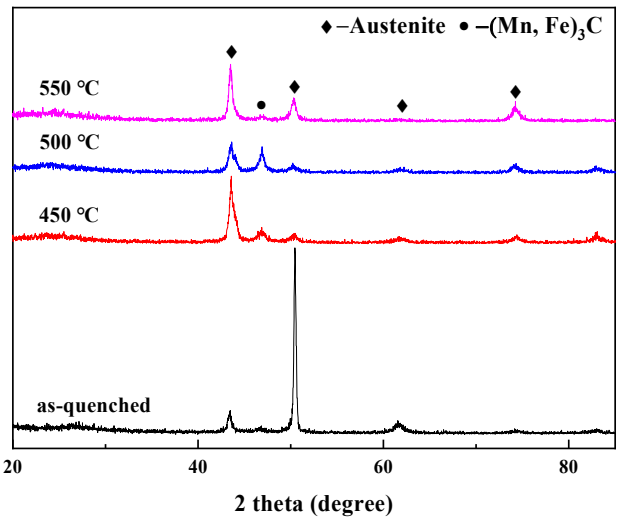

Figure 5. X-ray diffraction patterns of Mn25 aged at different aging temperatures.

3.3. Effect of Aging Temperature on Wear Characteristics and Work Hardening of High Manganese Steel

Figure 6 shows that the wear weight loss of Mn25 steel under different impact wear conditions. As shown in Figure 6a, in the low impact load (2.0 J) wear conditions, with the increase in aging temperature, wear loss of Mn25 steel was a decreasing trend. In addition, the wear loss of Mn25 steel at the aging temperature of 550 °C was significantly lower than the wear loss of Mn25 steel at an aging temperature of 450 °C and 500 °C; the abrasion resistance of Mn25 steel was the best. It can be seen in Figure 6b that when the wear conditions are in the high-impact load (5.0 J), the wear weight loss of Mn25 steel gradually decreases with the increase in aging temperature; while at aging temperatures of 450 °C and 500 °C, the wear weight loss of Mn25 steel is almost the same. When the aging temperature reaches up to 550 °C, a good combination of toughness and hardness exhibits in Mn25 steel that contributes to the superior impact wear resistance of Mn25 steel. It can be seen in Figure 6 that under high-impact load, the weight loss of high manganese steel without aging treatment is lower than that under low impact load; that is, the wear resistance of high manganese steel under high-impact load is higher than that under low impact load. The wear resistance of high manganese steel is greatly restricted by the working conditions. In high-impact contact abrasive wear, high manganese steel is easy to produce work hardening and improve wear resistance, and then it can reflect its wear characteristics [21–25].

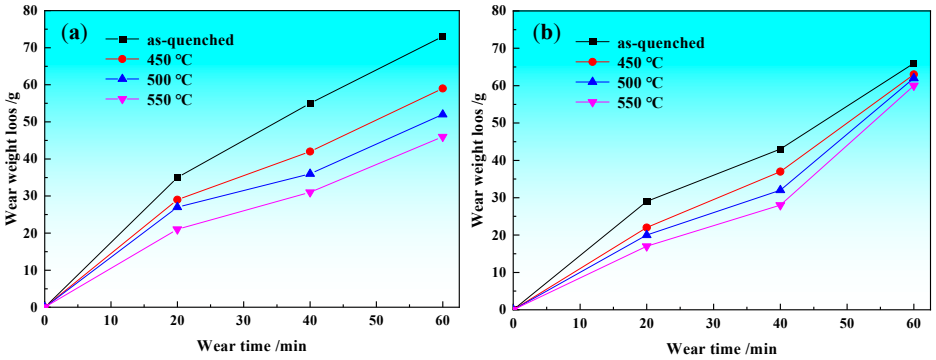

Figure 6. Wear weight loss of Mn25 steel under (**a**) low-energy impact 2.0 J and (**b**) high-energy impact 5.0 J at different wear times.

The impact abrasive wear of high manganese steel is different under different impact energy, which is related to the good work-hardening ability of high manganese steel. Hardness is one of the major properties that affects the wear resistance of materials [26,27]. Figure 7 shows the microhardness distribution of wear surfaces under high-impact loads (5.0 J). As shown in Figure 7, the surface hardness of the high manganese steel specimens showed a significant increase due to the hardening process; the highest hardness could reach up to 461.52 HV. When at an aging temperature of 550 °C, with an increase of 245 HV relative to the initial hardness, the percentage of hardening of the high manganese steel specimens is up to 49.96 percent, and the depth of the hardened layer is up to 3800 μm. For aging temperatures 450 °C and 500 °C, the affected layers are about 3000 μm and 3400 μm, respectively. As the aging temperature increases, the effective hardening layer of Mn25 steel becomes deeper, the microhardness value of the wear section increases significantly, and the magnitude of the increase in the microhardness of the wear section relative to the initial hardness value increases to varying degrees. A deeper affected layer means good wear resistance for the impact abrasive wear [28–30]. After aging treatment at 550 °C, the Mn25 steel shows excellent work-hardening ability and wear resistance.

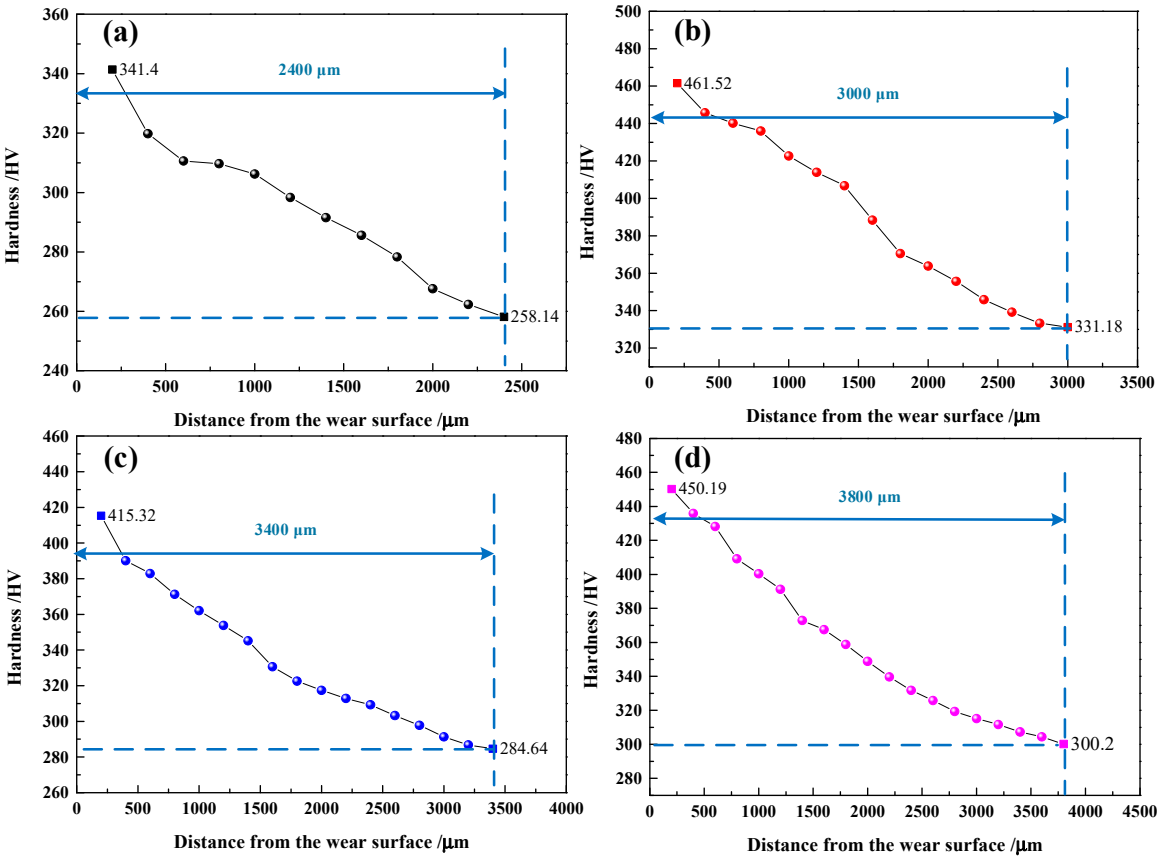

Figure 7. Microhardness distribution of wear surfaces under high-impact energy of 5.0 J (the dashed line refers to the surface hardness before friction test). (**a**) as-quenched, (**b**) 450 °C, (**c**) 500 °C, and (**d**) 550 °C.

3.4. Effect of Aging Temperature on Wear Mechanism of High Manganese Steel

Figure 8a–h shows morphologies of the worn surface of Mn25 steel at different impact energies. It can be seen in Figure 8a that press-in particles and furrows could be observed on the wear surface of Mn25 under the low impact energy of 2.0 J. Owing to the fact that the hardness of M25 steel is relatively low, abrasive particles are embedded into the surface. As shown in Figure 8b–d, no obvious press-in particle could be found on the wear surface

with the increase in aging treatment temperature. There are shallow cutting furrows on the surface, most of which are fatigue spalling, and the amount of spalling on the wear surface reduces when the temperature of the effect treatment is increased. When the impact energy increases up to 5 J, as shown in Figure 8e–h, a large number of abrasive particles are embedded into the surface. However, after the aging temperatures are higher than 500 °C, the press-in abrasive particles on the worn surface are significantly reduced, which is the result of high hardness and good work-hardening behavior. A hardening layer could be formed easily under the impact load. When the aging temperature is at 550 °C, the worn surface of Mn25 steel is smooth, and the wear resistance is better under both low and high-impact load. According to Figure 8, the wear mechanism of Mn25 steel under 2.0 J and 5.0 J impact-load wear conditions have plastic fatigue-spalling and micro-cutting at the same time; and, under low impact load of 2.0 J, the wear mechanism of Mn25 steel is mainly micro-cutting, and there are obvious directional cutting furrows. In high-impact load 5.0 J conditions, this time Mn25 steel mainly has a fatigue spalling wear mechanism. Ojala et al. found that work-hardening and mechanical performance have a significant effect on wear performance [31]. Comprehensive analysis, under the 2.0 J and 5.0 J impact work of abrasive wear conditions with the increase in aging temperature, is that, after wear 1 h the wear weight loss of Mn25 steel is smaller and its wear resistance is better. Under the 5.0 J impact power of abrasive wear conditions, the wear surface morphology of the Mn25 steel fatigue-spalling pit becomes shallower, indicating that the impact abrasive wear resistance of Mn25 steel is better.

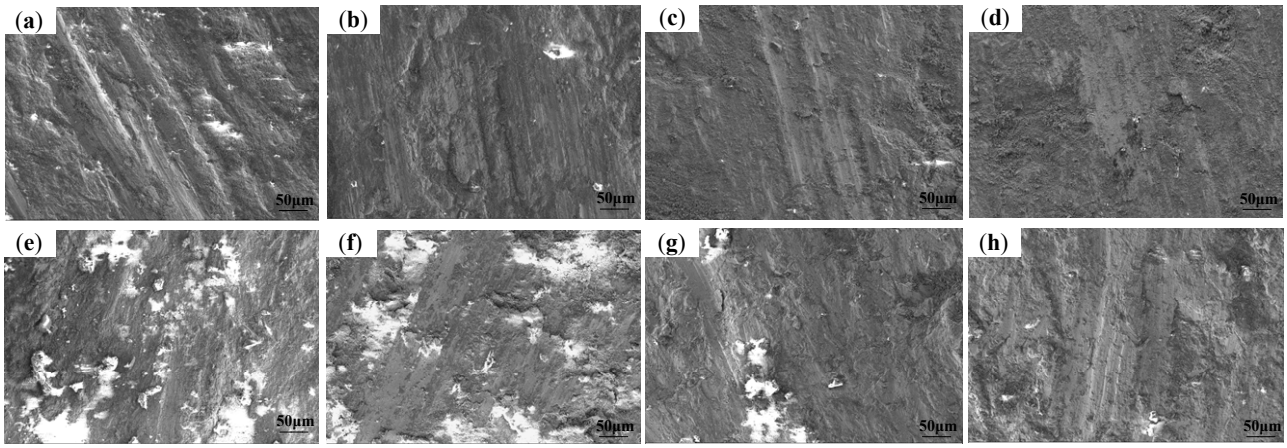

Figure 8. SEM morphologies of worn surface of Mn25 steel at different impact energies. (**a**–**d**) 2 J, (**e**–**h**) 5 J; (**a**,**e**) as-quenched, (**b**,**f**) 450 °C, (**c**,**g**) 500 °C, and (**d**,**h**) 550 °C.

For the abrasive wear behavior, the wear morphology is often caused by the joint action of a variety of mechanisms [31]. Based on the above results, the wear model of the experimental steel under impact wear conditions is summarized, and its schematic diagram is shown in Figure 9. In the process of impact wear, the specimen is mainly subjected to tangential and normal forces from abrasive particles. For the tangential force, furrows easily appear on the surface with high plasticity, and a surface with low plasticity and high hardness is easy to be micro-cut to produce chips. For the normal force, it mainly comes from the impact stress generated when the hammer falls, which, on the one hand, causes the abrasive particles to embed into the surface and form the crack source. On the other hand, due to the continuous impact, such repeated plastic deformation eventually led to the peeling of the material, which became debris.

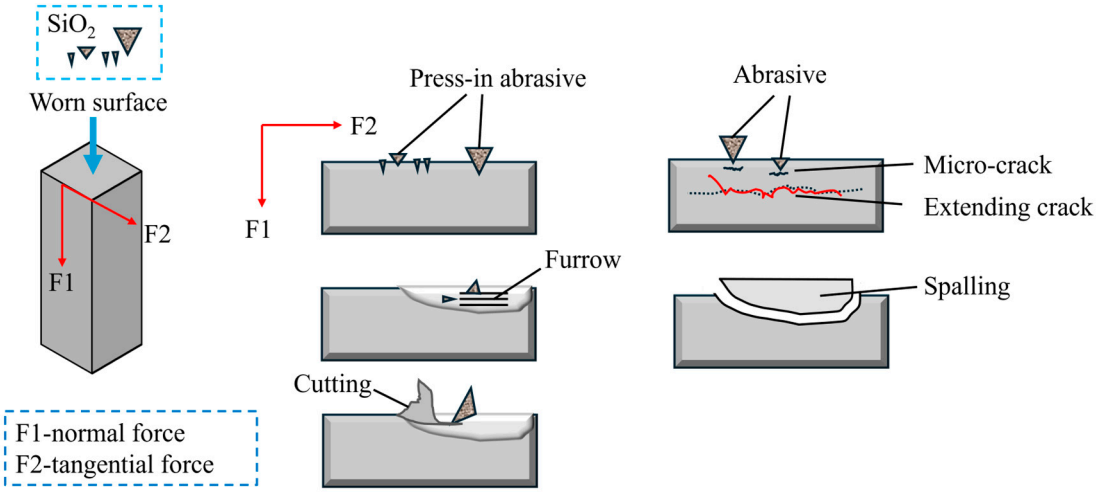

Figure 9. Schematic diagram of wear model of Mn25 steel under impact wear condition.

4. Conclusions

(1) With the aging temperature increases, the impact toughness first sharply reduced and then increased, while the corresponding hardness was first increased and then decreased. When the aging temperature is 400 °C, the surface hardness of Mn25 steel reaches the maximum value 331.16 HV, while its impact toughness value is the smallest at 153.92 J. When the aging temperature is 550 °C, the impact toughness and hardness match better. Combining the XRD patterns, the precipitation phase is uniformly dispersed in the matrix, which can improve the initial hardness of high manganese steel, while the toughness is not reduced.

(2) Under different impact wear conditions, with the increase in aging temperature, wear loss of Mn25 steel was a decreasing trend. As the aging temperature increases, the effective hardening layer of Mn25 steel becomes deeper, the microhardness value of the wear section increases significantly, and the magnitude of the increase in the microhardness of the wear section relative to the initial hardness value increases to varying degrees. Under 5.0 J high-impact load abrasive wear conditions, when at an aging temperature of 550 °C, with an increase of 245 HV relative to the initial hardness, the percentage of hardening of the high manganese steel specimens is up to 49.96 percent, and the depth of the hardened layer is up to 3800 μm. For aging temperatures of 450 °C and 500 °C, the affected layers are about 3000 μm and 3400 μm, respectively.

(3) For Mn25 steel in different impact load conditions, its wear mechanism is micro-cutting and fatigue-spalling at the same time. Specifically, under 2.0 J low impact load abrasive wear conditions, Mn25 steel wear is dominated by micro-cutting; with the aging temperature increases, the degree of steel wear hardening increases, and micro-cutting resistance is stronger. Under 5.0 J high impact load abrasive wear conditions, the Mn25 steel wear tends to plastic fatigue-spalling; with the aging temperature increases, the degree of steel wear hardening and the toughness of the wear layer and subsurface layer increases. When at an aging temperature of 550 °C, the wear surface morphology of Mn25 steel fatigue-spalling pit is shallow, which shows better wear resistance. This is related to the better matching of hardness and impact toughness of Mn25 steel after aging treatment, as well as better work-hardening ability.

Author Contributions: Conceptualization, X.H. and X.Q. (Xiya Qiao); methodology, X.H., X.Q. (Xiangyu Qi), X.Y. and Y.X.; software, X.Q. (Xiya Qiao), L.Y. and Y.X.; validation, X.Q. (Xiya Qiao), L.Y. and X.H.; formal analysis, X.Q. (Xiya Qiao), L.Y., X.H. and X.Q. (Xiangyu Qi); investigation, X.Q.

(Xiya Qiao), X.Y. and Y.X.; resources, X.H. and X.Q. (Xiangyu Qi); data curation, X.Q. (Xiya Qiao), L.Y. and X.Y.; writing—original draft preparation, X.Q. (Xiya Qiao); writing—review and editing, L.Y. and X.H.; visualization, X.Q. (Xiya Qiao); supervision, X.H.; project administration, X.H.; funding acquisition, X.H. All authors have read and agreed to the published version of the manuscript.

Funding: This work was financially supported by Joint Fund Project of State Key Laboratory of Metal Material for Marine Equipment and Application (HGSKL-USTLN (2021) 10).

Data Availability Statement: The original contributions presented in this study are included in the article. Further inquiries can be directed to the corresponding author.

Acknowledgments: The authors thank team partners from the key laboratory of green low-carbon and intelligent metallurgy of Liaoning province for their valuable contribution to this work and preparation of this paper.

Conflicts of Interest: The authors declare that they have no known competing financial interests or personal relationships that could have appeared to influence the work reported in this paper.

References

1. Wen, Y.H.; Peng, H.B.; Si, H.T.; Xiong, R.; Raabe, D. A novel high manganese austenitic steel with higher work hardening capacity and much lower impact deformation than Hadfield manganese steel. *Mater. Des.* **2014**, *55*, 798–804. [CrossRef]
2. El Fawkhry, M.K. Feasibility of new ladle-treated Hadfield steel for mining purposes. *Int. J. Miner. Metall. Mater.* **2018**, *25*, 300–309. [CrossRef]
3. Efstathiou, C.; Sehitoglu, H. Strain hardening and heterogeneous deformation during twinning in Hadfield steel. *Acta Mater.* **2010**, *58*, 1479–1488. [CrossRef]
4. Barbangelo, A. Influence of alloying elements and heat treatment on impact toughness of chromium steel surface deposits. *J. Mater. Sci.* **1990**, *25*, 2975–2984. [CrossRef]
5. Scott, C.; Remy, B.; Collet, J.L.; Cael, A.; Bao, C.; Danoix, F.; Malard, B.; Curfs, C. Precipitation strengthening in high manganese austenitic TWIP steels. *Int. J. Mater. Res.* **2011**, *102*, 538–549. [CrossRef]
6. Reyes-Calderón, F.; Mejía, I.; Boulaajaj, A.; Cabrera, J. Effect of microalloying elements (Nb, V and Ti) on the hot flow behavior of high-Mn austenitic twinning induced plasticity (TWIP) steel. *Mater. Sci. Eng. A* **2013**, *560*, 552–560. [CrossRef]
7. Feng, X.Y.; Zhang, F.C.; Yang, Z.N.; Zhang, M. Wear behaviour of nanocrystallised Hadfield steel. *Wear* **2013**, *305*, 299–304. [CrossRef]
8. Beheshti, M.; Zabihiazadboni, M.; Ismail, M.C.; Kakooei, S.; Shahrestani, S. Investigation on simultaneous effects of shot peen and austenitizing time and temperature on grain size and microstructure of austenitic manganese steel (Hadfield). *IOP Conf. Ser. Mater. Sci. Eng.* **2018**, *328*, 012006.
9. Meng, S.; Cui, C.Y.; Chen, K.; Zhao, K. Microstructure and mechanical properties of laser-shock-peened high-manganese steel. *Electroplat. Finish.* **2020**, *39*, 760–765.
10. Hu, X.; Shen, Z.; Liu, Y.; Liu, T.; Wang, F. Influence of explosive density on mechanical properties of high manganese steel explosion hardened. *J. Appl. Phys.* **2013**, *114*, 213507. [CrossRef]
11. Wang, Z.; Yang, Y.; Chen, C.; Li, Y.; Yang, Z.; Lv, B.; Zhang, F. Effect of surface impacting parameters on wear resistance of high manganese steel. *Coatings* **2023**, *13*, 539. [CrossRef]
12. Zhou, Z.; Zhang, Z.; Shan, Q.; Li, Z.; Jiang, Y.; Ge, R. Influence of heat-treatment on enhancement of yield strength and hardness by Ti-V-Nb alloying in high-manganese austenitic steel. *Metals* **2019**, *9*, 299. [CrossRef]
13. Feng, Y.; Song, R.; Peng, S.; Song, R. Microstructures and impact wear behavior of Al-alloyed high-Mn austenitic cast steel after aging treatment. *J. Mater. Eng. Perform.* **2019**, *28*, 4845–4855. [CrossRef]
14. Lee, K.; Park, S.J.; Lee, J.; Moon, J.; Kang, J.Y.; Kim, D.I.; Suh, J.Y.; Han, H.N. Effect of aging treatment on microstructure and intrinsic mechanical behavior of Fe-31.4 Mn-11.4 Al-0.89 C lightweight steel. *J. Alloys Compd.* **2016**, *656*, 805–811. [CrossRef]
15. Feng, Y.; Song, R.; Wang, Y.; Liu, M.; Li, H.; Liu, X. Aging hardening and precipitation behavior of Fe-31.6 Mn-8.8 Al-1.38 C austenitic cast steel. *Vacuum* **2020**, *181*, 109662. [CrossRef]
16. Shin, J.H.; Rim, G.Y.; Kim, S.D.; Jang, J.H.; Park, S.-J.; Lee, J. Effects of aging heat-treatment on dynamic strain aging behavior in high-Mn lightweight steel. *Mater. Charact.* **2020**, *164*, 110316. [CrossRef]
17. Shan, Q.; Zhang, T.; Li, Z.; Zhou, Z.; Jiang, Y.; Lee, Y.S.; Luo, X. Effect of Aging Treatment on Precipitates and Intrinsic Mechanical Behavior of Austenitic Matrix in Ti-V-Nb-Alloyed High-Manganese Steel. *Steel Res. Int.* **2021**, *92*, 2000650. [CrossRef]

18. Ren, J.; Li, Z.; Zhou, X.; Wu, S.; Chen, J.; Liu, Z. Interpretation of microstructure evolution and mechanical properties under aging treatments of a Fe–24Mn-0.6 C–2Al-0.6 V austenitic steel for cryogenic application. *J. Mater. Res. Technol.* **2023**, *24*, 4661–4677. [CrossRef]
19. *GB/T 229-2020*; Metallic Materials—Charpy Pendulum Impact Test Method. Standards Press of China: Beijing, China, 2021.
20. Peng, S.; Song, R.; Sun, T.; Pei, Z.; Cai, C.; Feng, Y.; Tan, Z. Wear behavior and hardening mechanism of novel lightweight Fe–25.1 Mn–6.6 Al–1.3 C steel under impact abrasion conditions. *Tribol. Lett.* **2016**, *64*, 13. [CrossRef]
21. Babichev, M.A.; Velikanova, A.A. Effect of the concentration of manganese on the wearability of steel. *Met. Sci. Heat Treat.* **1964**, *6*, 289–292. [CrossRef]
22. Primig, S.; Leitner, H. Transformation from continuous-to-isothermal aging applied on amaraging steel. *Mater. Sci. Eng.* **2010**, *527*, 4399–4405. [CrossRef]
23. Bouaziz, O.; Allain, S.; Scott, C.P.; Cugy, P.; Barbier, D. High manganese austenitic twinning induced plasticity steels: A review of the microstructure properties relationships. *Solid State Mater. Sci.* **2011**, *15*, 141–166. [CrossRef]
24. Mazancová, E.; Ružiak, I.; Schindler, I. Influence of rolling conditions and aging process on mechanical properties of high manganese steels. *Arch. Civ. Mech. Eng.* **2012**, *12*, 142–147. [CrossRef]
25. Petrov, Y.N.; Gavriljuk, V.G.; Berns, H.; Schmalt, F. Surface structure of stainless and Hadfield steel after impact wear. *Wear* **2005**, *260*, 687–691. [CrossRef]
26. Efremenko, V.G.; Shimizu, K.; Noguchi, T.; Efremenko, A.; Chabak, Y.G. Impact–abrasive–corrosion wear of Fe-based alloys: Influence of microstructure and chemical composition upon wear resistance. *Wear* **2013**, *305*, 155–165. [CrossRef]
27. Ba, L.; Gao, Q.; Cen, W.; Wang, J.; Wen, Z. The impact-abrasive wear behavior of high wear resistance filling pipeline with explosion treatment. *Vacuum* **2021**, *192*, 110427. [CrossRef]
28. Guo, Y.; Wang, Y.; Ma, Z.; Han, J. Microstructure Characteristic and Impact Wear Behavior of Nb-Alloyed High Manganese Steels. *J. Mater. Eng. Perform.* **2023**, *32*, 9040–9050. [CrossRef]
29. Ma, H.; Chen, C.; Li, J.; Wang, X.; Qi, X.; Zhang, F.; Tang, T. Effect of pre-deformation degree on tensile properties of high carbon high manganese steel at different strain rates. *Mater. Sci. Eng. A* **2022**, *829*, 142146. [CrossRef]
30. Bedolla-Jacuinde, A.; Guerra, F.V.; Rainforth, M.; Mejía, I.; Maldonado, C. Sliding wear behavior of austempered ductile iron microalloyed with boron. *Wear* **2015**, *330*, 23–31. [CrossRef]
31. Khun, N.W.; Liu, E.; Tan, A.W.Y.; Senthilkumar, D.; Albert, B.; Lal, D.M. Effects of deep cryogenic treatment on mechanical and tribological properties of AISI D3 tool steel. *Friction* **2015**, *3*, 234–242. [CrossRef]